

Kinetostatic Design Considerations for an Articulated Leg-Wheel Locomotion Subsystem

Seung Kook Jun

Glenn D. White

Venkat N. Krovi¹

Mechanical & Aerospace Engineering,
State University of New York at Buffalo,
Buffalo, NY 14260

Our long-term goal is one of designing land-based vehicles to provide enhanced uneven-terrain locomotion capabilities. In this paper, we examine and evaluate candidate articulated leg-wheel subsystem designs for use in such vehicle systems. The leg-wheel subsystem designs under consideration consist of disk wheels attached to the chassis through an articulated linkage containing multiple lower-pair joints. Our emphasis is on creating a design that permits the greatest motion flexibility between the chassis and wheel while maintaining the smallest degree-of-freedom (DOF) within the articulated chain. We focus our attention on achieving two goals: (i) obtaining adequate ground clearance by designing the desired/feasible motions of the wheel axle, relative to the chassis, using methods from kinematic synthesis; and (ii) reducing overall actuation requirements by a judicious mix of structural equilibration design and spring assist. This process is examined in detail in the context of two candidate single-degree-of-freedom designs for the articulated-leg-wheel subsystems—a coupled-serial-chain configuration and a four-bar configuration. We considered the design synthesis of planar variants of the two candidate designs surmounting a representative obstacle profile while supporting a set of end-effector loads and highlight the key benefits in the presented results.

[DOI: 10.1115/1.2168481]

1 Introduction

In recent years, there has been considerable interest in creation of land-based locomotion systems for operation on rough unprepared surfaces. Such systems have found numerous applications in a wide variety of arenas such as exploration of extraterrestrial [1–3], extreme terrestrial [4–6], and disaster environments [7]. While high mobility, obstacle-surmounting capability and maneuverability are the obvious major requirements, additional criteria such as robustness, reliability, and efficiency are also extremely desirable.

Legged locomotion systems have been the preferred solution for maneuvering on such rough/unprepared terrain [8,9] due to their ability to pick and choose their footholds and the natural suspension provided by the articulations. This versatility, however, comes at the cost of increased power consumption requirements, making legged systems nonviable in environments with a limited power supply. In contrast, wheeled systems have been the de-facto design standard for most land-based locomotion systems due to the passive nature of the support and overall energy efficiency [10,11]. The limitation of wheeled systems, however, is that they function best on hard, prepared surfaces, which can provide continuous nonslipping support for rolling wheels [12].

In this paper, we will examine the creation of articulated leg-wheel subsystems of the type shown in Fig. 1, in order to combine the benefits of both legged and wheeled systems. The leg-wheel subsystem designs consist of articulated linkages with multiple lower pair joints (revolute/prismatic) between the wheel and the chassis. Numerous variants of such designs are possible depend-

ing upon the type, number, sequencing and nature of actuation (active/passive) of the joints. Examples range from the Mars Rover [1,2] and SHRIMP with rocker bogie suspensions [3], the NOMAD [4] and other wheeled actively articulated vehicle (WAAV) [13] designs with articulated frames, to systems like the Work Partner [5,6], Roller-Walker [14,15], and ALDURO [16] with powered legs and active/passive wheels. In almost all these cases, it is the addition of articulations in the mechanical design that endows them with their superior locomotion capabilities. However, in almost all cases no systematic effort to “design” the articulated leg-wheel system is ever considered.

This need for a systematic design process is motivated qualitatively using the example of a vehicle closely resembling the SHRIMP [3] surmounting a step. Nominal parameters were obtained and two virtual prototype variants were developed, as shown in Fig. 2. The sole difference between the two is in terms of the geometry of the front four-bar leg-wheel mechanism (a difference that is difficult to distinguish at first glance). Both virtual prototypes were then numerically simulated (at high resolution) under identical conditions with dramatically different outcomes also seen in Fig. 2. Despite the qualitative nature, this example is illustrative from many viewpoints. On one hand, it makes a case for using a simulation based design process for refining a design using the usual designer prerogatives (intuition and trial and error). On the other hand, it also makes a case for systematic application of mechanism design principles to aid performance enhancements as well as sensitivity analysis. It is this latter systematic approach that we will explore further in this paper.

In general, any such design process must take into account innumerable, often equally important, considerations such as the loss of stability, tip-over stability and ground traction for the task of locomotion on uneven terrain. However, in this paper, we will specifically focus our attention on two major complementary/conflicting design criteria—workspace and suspension—in creating candidate designs for such articulated leg-wheel systems. A

¹Corresponding author.

Contributed by the Dynamic Systems, Measurement, and Control Division of ASME for publication in the JOURNAL OF DYNAMIC SYSTEMS, MEASUREMENT, AND CONTROL. Manuscript received March 10, 2005; final manuscript received November 22, 2005. Review conducted by Suhada Jayasuriya. Paper presented at the 2004 ASME International Mechanical Engineering Congress (IMECE 2004), November 13–19, 2004, Anaheim, California, USA.

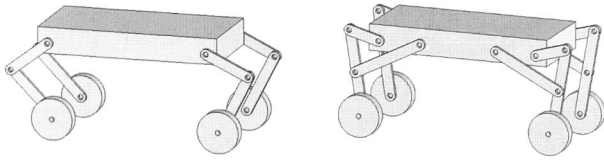


Fig. 1 Artist's conceptions of articulated leg-wheel based locomotion systems

large work space is desirable from the viewpoint of achieving adequate ground clearance and the ability to surmount obstacles. In such situations, the open-kinematic structure of serial-chain based systems would be a natural choice. In contrast, typical suspension designs feature an extremely small work space and highly stiff articulations with minimal actuation requirements. Traditionally, in such situations, various types of closed-loop mechanical linkages have played an important role. A systematic selection between such competing criteria is one of the underlying themes in our work. We begin this process by considering two performance criteria—*articulated degrees of freedom* (DOF) and *equilibration*—to help us characterize these many variants of the designs.

Articulated Degrees-of-Freedom. In the sagittal plane, the wheel axle frame has two translation degrees of freedom (DOF) relative to chassis, as shown in Fig. 3 (since the orientation of the wheel rolling about its axis is irrelevant). However, a designer can control the number of DOF that are retained/eliminated by changing types of articulations/joints (and the links) of the intermediate mechanism. This can range from: (i) eliminating all DOF by introducing a rigid connection; (ii) retaining one DOF by introducing a single lower-pair joint; and (iii) retaining the full two DOF by introducing at least two lower-joint pairs as shown in Fig. 3.

Equilibration. Adding additional articulations increases the intermediate degree of freedom within the chain, which need to be controlled/restricted either: (i) *actively* by actuation, (ii) *semi-actively* using springs and dampers; or (iii) *passively* by adding some form of structural equilibration using hardware constraints. Since the load-bearing requirements can be significant, we will focus on the use of structural equilibration to bear these loads to the largest extent possible. The partitioning of the load bearing is highly configuration dependent and we will examine ways of customizing the configuration to enhance this process. Subsequently,

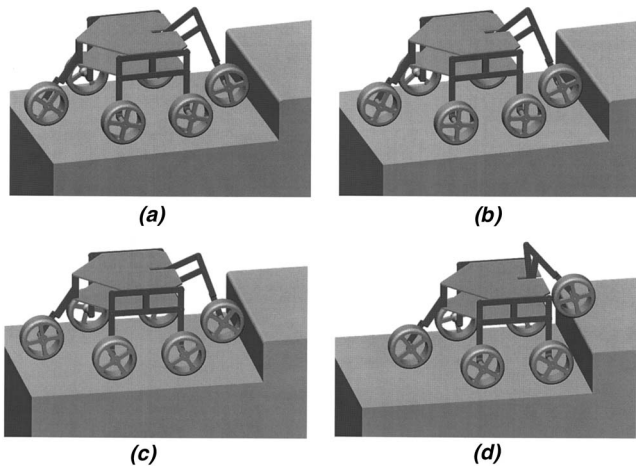


Fig. 2 (a), (b) Start and end of simulation with first four-bar design. Climbing of the step was unsuccessful. (c), (d) Start and end of simulation with second four-bar design. Climbing of the step was successful.

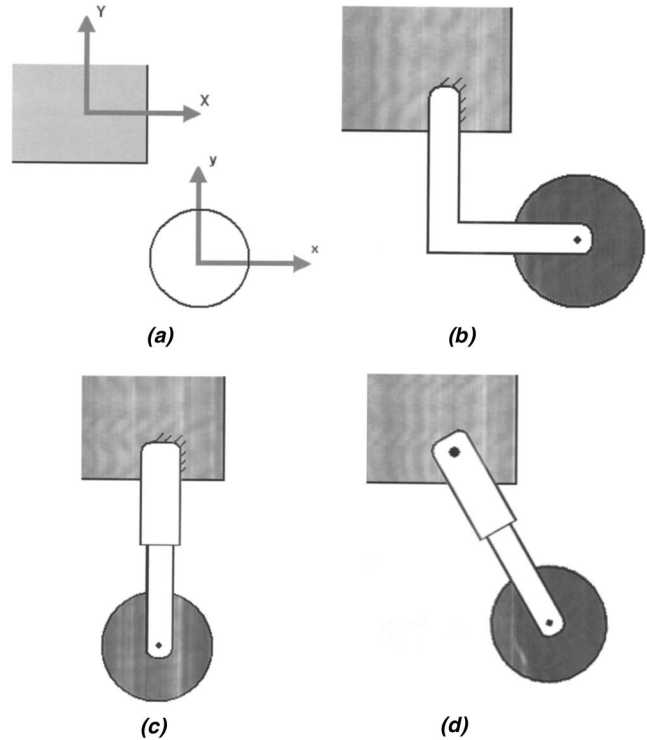


Fig. 3 (a) The chassis and wheel frames with two relative DOF and corresponding articulations with (b) zero DOF; (c) one DOF; and (d) two DOF

we will also examine the use of spring assists to further reduce the overall actuation requirements.

1.1 Single Degree-of-Freedom Articulated Leg-Wheel Systems.

The simplest form of a single degree-of-freedom articulated leg-wheel system design is a single link with a simple lower-pair joint. However, simple articulations such as these have very limited geometric motion capability, e.g., a revolute joint would limit the wheel-axle to move in a circle while a prismatic joint would constrain it to move in a straight line. Our emphasis in the selection process, therefore, will be on an articulated leg-wheel system design that permits the wheel axle to trace a complex geometric motion trajectory relative to the chassis while maintaining the smallest DOF within the articulated chain.

Typically more joints must be added to increase the DOF within the chain in order to permit tracing curves of greater complexity. Constraints are then added to the system in order to restrict the wheel-axle to a desired trajectory. Such constraints can be implemented either passively using hardware elements or actively by way of software control. In our work, we will make a case for creating *passive* articulated mechanical subsystems with built-in capability for graceful system degradation to a less capable (but stable) operational mode in cases of power failure. In particular, we will focus on two candidate designs which employ passive constraint implementation using hardware.

- The first candidate design employs the coupled serial chain (CSC) configuration, as shown in Fig. 4(b). Such a configuration is obtained by physically coupling the distal joint rotations of a revolute-jointed, multi-link, serial chain mechanism to the rotation of the proximal joint resulting in a single degree-of-freedom coupled serial chain (SDCSC) mechanism. The rotation of the base link now drives all the other coupled links and increasing the number of links enables us to trace curves of increasing

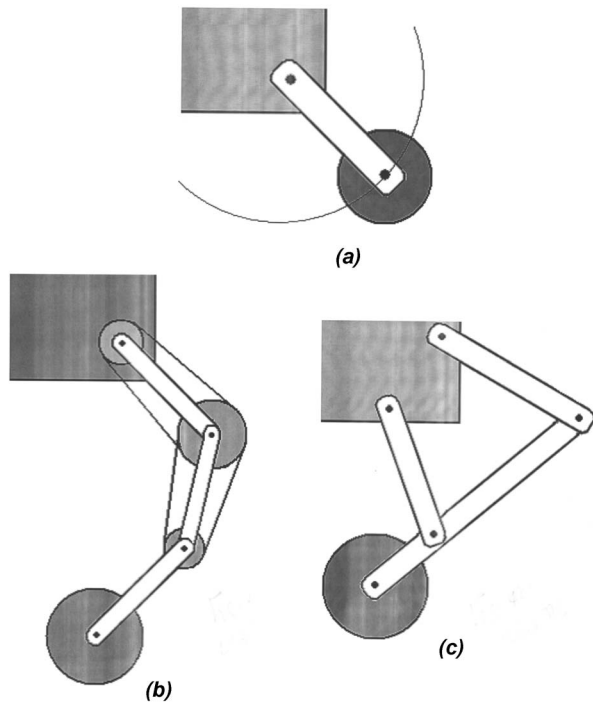


Fig. 4 Constrained single degree-of-freedom motions can be achieved using: (a) a single lower-pair articulation, or multiple articulations but with suitable hardware constraints in (b) a single degree-of-freedom coupled serial chain (SDCSC) or (c) a four-bar configuration

complexity and variety while retaining the single degree-of-freedom operation [17,18].

- The alternate design is one that uses the well-known four-bar configuration as shown in Fig. 4(c). The four-bar linkage is the simplest possible pin-jointed mechanism for single degree-of-freedom motion while allowing tracing of geometrically complex motion and force-profiles—this versatility is responsible for its ubiquitous use in machinery designs [19,20].

In this paper, we will emphasize the design customization and adaptation of these two single DOF designs for use on rough terrain to: (i) tackle increasing terrain roughness, and (ii) reduce actuation requirements. The rest of the paper is organized as follows: Sec. 2 provides a brief background of the general kinetostatic design approach adopted. Sections 3 and 4 leverage this framework for kinetostatic design optimization for the cases of the SDCSC-based and four-bar-based leg-wheel subsystems, respectively. Finally, concluding remarks and a discussion are presented in Sec. 5.

2 Design Approach

2.1 Combined Precision-Point Synthesis & Optimization.

The general design problem is formulated in the framework of dimensional synthesis of mechanisms [17–20]. In particular, given a set of task specifications and the type of mechanism, an optimization problem can be formulated to determine the set of parameters to match desired specifications. This process offers a systematic means for selection of large sets of unknown parameters. However, the resulting solutions satisfy all these desired specifications only in the least-squares sense without guaranteeing exact satisfaction of any specification.

Greater structure is added to this problem by employing precision point synthesis. The requirement to match specifications exactly at precision points creates constraints between the various

mechanism design parameters, which helps in the final selection of design parameters. These constraints can be combined within the aforementioned optimization-based framework to create a constrained design optimization problem. This is the well known approach used for mechanism synthesis, where such constraints are typically derived solely from kinematic considerations and reintegrated into the optimization problem using a penalty formulation.

In contrast, in this paper, we will make a case for developing and using additional constraints relating the joint actuation and the end effector forces by application of the principle of virtual work to the articulated subsystem [17,18]. Further, we also adopt an approach for solving the constrained optimization problem that emphasizes: (i) the partial specification of design requirements on the end effector; (ii) a suitable partitioning of all the variables into dependent and independent variables; and (iii) explicit creation/solution of a linear system of equations in terms of the independent variables. Optimization over the independent variables yields different candidate mechanisms, which satisfies the design specifications exactly at the selected precision points and in the least-squares sense elsewhere. The principal advantage of this approach is the ability to add structure to the problem while offering adequate flexibility/choices to the designer. Further, we note that other types of design specifications can also be explored in addition to the ones used in this paper.

2.2 Kinetostatic Design of the Leg-Wheel Subsystem.

The design of an articulated leg-wheel system that is capable of surmounting an obstacle using minimal actuation forces offers many challenges. Suitable selection of various mechanism parameters is critical and includes both *kinematic* parameters, such as the link lengths and initial configuration, as well as *static* parameters such as spring constants and their preloads.

The overall problem may be considered as a merger of two interlinked stages. The kinematic stage entails the selection of the parameters to permit the wheel axle (which serves as the end effector) to follow a desired pre-specified path relative to the chassis (which serves as the base). However, the force interaction between a linkage and its environment also becomes critical to the performance (as in the case of our leg-wheel design). In this case, the goal of the articulation is to guide the attached wheel axle through several positions while supporting a *set of specified external loads*. Hence, in this stage we examine the kinetostatic design process for the selection of the optimal parameters to support these external loads to the largest extent by *structural equilibration*. Building on the work presented in [17,18], we also consider the addition of torsional springs to each joint to further minimize/optimize the peak actuator torques by using a judicious combination of *structural equilibration* and *spring assist* design.

In general, the above problem entails a simultaneous determination of optimal mechanism and spring parameters, as shown in Fig. 5. However, for the discussion in the next two sections, we will assume that the optimal mechanism parameters have been computed previously in a kinematic stage. This enables us to focus solely on the determination of the spring parameters to satisfy the desired static constraints in the static stage, as shown in Fig. 6. The interested reader is referred to [21] for further details.

2.3 Specific Test Scenario.

In this paper, we will consider an ideal step profile determined using the uniform building codes to have a tread of 0.241 m (9.5 in.) and a rise of 0.191 m (7.5 in.). In general, the specification of a desired kinematic motion curve consists of both the motion of the axle with respect to a chassis frame and motion of the chassis frame itself. However, without loss of generality, we will nominally assume a fixed chassis for the rest of this paper. The designer has freedom in selecting the type, number, and locations of the precision points at which an exact matching of the motion trajectories is desired. Up to three precision points may be selected without foregoing the linear solution process described in Sec. 3.1. For convenience we select

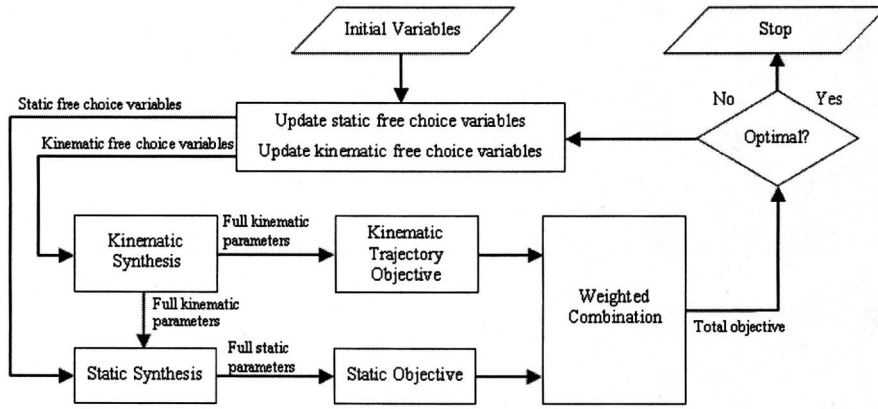


Fig. 5 Coupled kinetostatic synthesis to match desired motion and force specifications

them to be the start, middle, and end of the motion.

The geometry of the wheel and step places restrictions on the locations of the precision points. For example, the first precision point (the start point) must be at least one wheel radius from the ground while the third precision point (the end point) must be a similar one wheel radius height above the step. The ideal position for the start point would be when the wheel encounters the step and similarly an ideal finish point would be the top edge of the step. The intermediate point can now be selected based on convenience and can be used to control the shape of the trajectory. Figure 7 shows the candidate kinematic profile.

The mechanism motion causes the wheel to have intermittent contact with the ground as the step transition occurs—breaking contact when the step is encountered and reestablishing contact after surmounting the step—as seen in Fig. 8(a). The sample resulting wheel-axle force profile in Fig. 8(a) reflects this transition—the x component of the wheel-axle force rises briefly as the step is encountered and the y -component decreases to zero as lift-off is achieved. As the wheel comes back in contact with the step, the y component of the force rises to its final value and the x component remains zero.

Figure 8(b) depicts a candidate normalized desired actuator torque specification to be used to generate this motion independent of the loading conditions of Fig. 8(a). While the kinetostatic design process can potentially be used to match (most) any candidate torque profile, we wanted to emphasize several desirable features in the variant shown. The overall motion is depicted as being parameterized to lie between $\phi=0$ and $\phi=1$. The stable equilibrium near $\phi=0$ allows the wheel-axle to be robust to small load disturbances. However, if the actuated joint is moved past the unstable equilibrium at $\phi=0.1$, the system torques would aid the natural transition to the next equilibrium state at $\phi=1$. Other de-

sired torque profiles may similarly be created and the goal now becomes one of designing the static parameters of the system to achieve as close a match as possible.

3 Design/Synthesis of SDCSC Leg-Wheel Mechanism

3.1 Kinematic Synthesis. We select the desired trajectory for the wheel-axle to be one that can surmount the standard step described in Sec. 2.3 (see Fig. 9). The overall kinematic design selection problem may be expressed in the form of a constrained optimization problem as

$$\min_{\phi_2, \phi_3, R_1, R_2} \sum_{k=1}^{N_c} [(P_{x,k} - Q_{x,k})^2 + (P_{y,k} - Q_{y,k})^2] \quad (1)$$

subject to

$$\begin{bmatrix} \mathbf{Z}_1 \\ \mathbf{Z}_2 \\ \mathbf{Z}_3 \end{bmatrix} = \begin{bmatrix} 1 & 1 & 1 \\ e^{i\phi_2} & e^{iR_1\phi_2} & e^{iR_2\phi_2} \\ e^{i\phi_3} & e^{iR_1\phi_3} & e^{iR_2\phi_3} \end{bmatrix}^{-1} \begin{bmatrix} \mathbf{Z}_{P_1} - \mathbf{Z}_0 \\ \mathbf{Z}_{P_2} - \mathbf{Z}_0 \\ \mathbf{Z}_{P_3} - \mathbf{Z}_0 \end{bmatrix}$$

$$\phi_{\min} \leq \phi_2 \leq \phi_{\max}, \quad \phi_{\min} \leq \phi_3 \leq \phi_{\max}, \quad \phi_{\min} > 0 \quad (2)$$

$$R_{1,\min} \leq R_1 \leq R_{1,\max}, \quad R_{2,\min} \leq R_2 \leq R_{2,\max}$$

where $\mathbf{Q}_k = Q_{x,k} + iQ_{y,k}$ and $\mathbf{P}_k = P_{x,k} + iP_{y,k}$ correspond to the k th desired and actual position of the end effector at N_c discrete correspondence points along the curve. The design variables correspond to the incremental base rotation angles ϕ_2 and ϕ_3 at the second and third kinematic precision points, as shown in Fig. 9, and the two pulley ratios R_1 and R_2 . These are further constrained to satisfy physical realization. Furthermore, the position vector of

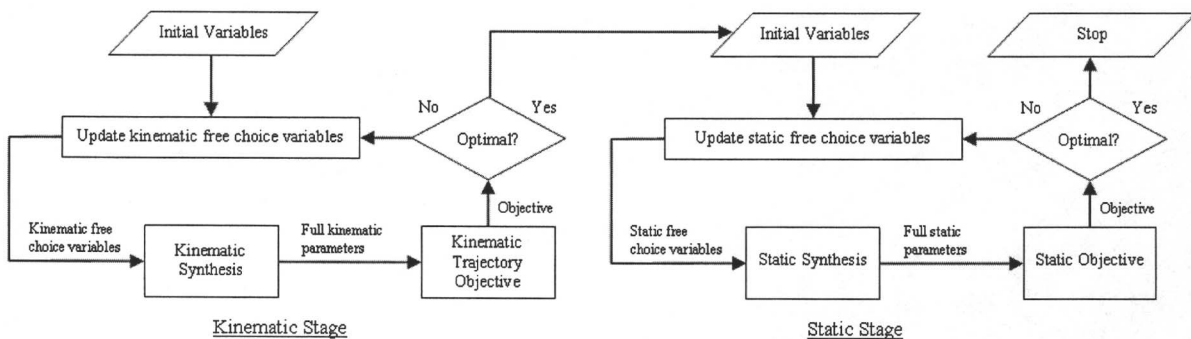


Fig. 6 Decoupled kinetostatic synthesis with a kinematic stage and a static stage

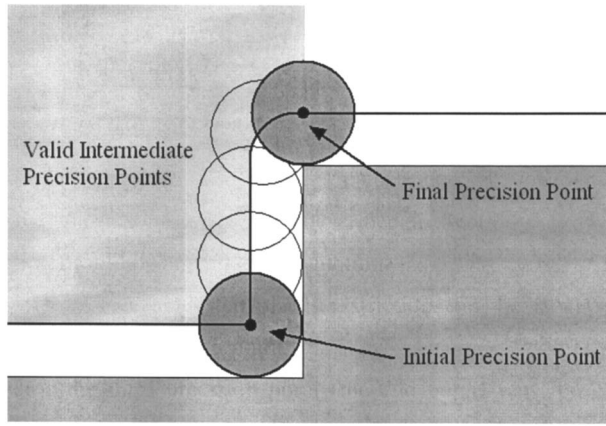


Fig. 7 Candidate kinematic profile and precision points for the wheel axle selected so as to surmount the step

the base joint, $\mathbf{Z}_0 = Z_{0x} + iZ_{0y}$, is fixed with respect to the chassis, and length of the first link is bounded to satisfy realization requirements. Note that the constraint equations corresponding to the kinematic precision point synthesis are derived by evaluating the forward kinematic equations at each precision point. Figure 10 shows the various kinematic configurations of the mechanism that surmount the step—in bold at the initial and final configurations and in lighter color along the rest of the curve. The parameters of the final optimized three-link SDCSC mechanism that traces the curve in Fig. 10 are shown in Table 1.

3.2 Kinetostatic Synthesis. The constraints on the static torque are derived from the principle of virtual work for every precision position. The actual torque, $T_1(\phi)$, applied at the base joint can be divided into two parts: (i) the torque required to equilibrate the external load, T_{Ext} , and (ii) the contribution of the

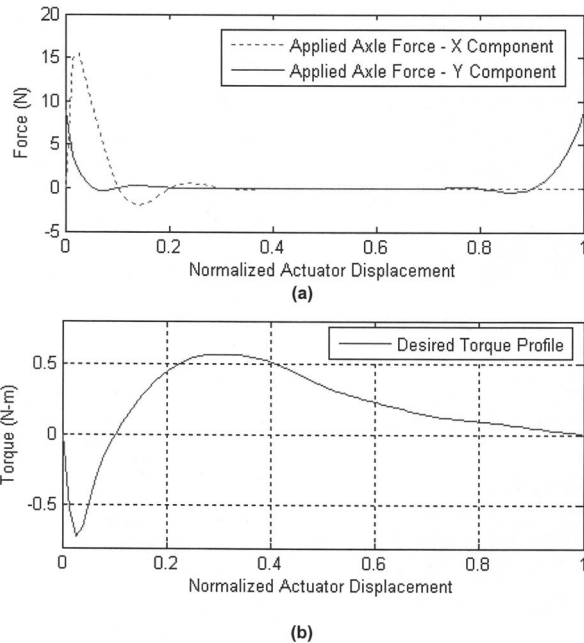


Fig. 8 Static force profile of the wheel axle traveling along the kinematic trajectory of Fig. 7 including: (a) candidate end-effector load applied at the wheel axle and (b) candidate desired torque profile intended to generate the motion

Table 1 Parameters of the optimized three-link SDCSC

Parameter	Value	Parameter	Value
Z_{0x}	-0.2290 m	Z_{0y}	0.1530 m
Z_{1x}	0.1700 m	Z_{1y}	-0.0504 m
Z_{2x}	0.0028 m	Z_{2y}	-0.0761 m
Z_{3x}	0.0045 m	Z_{3y}	0.0250 m
R_1	-5.85	R_2	-4.00
ϕ_{max}	44.0 deg		

internal spring torques, T_{Spr} , that can help reduce the overall required actuation, $T_1 = T_{\text{Ext}} - T_{\text{Spr}}$. The torque required to equilibrate the external load, T_{Ext} , can be expressed as

$$T_{\text{Ext}} = [A_1 \ A_2 \ A_3 \ A_4 \ A_5 \ A_6] \begin{bmatrix} z_{1x} \\ z_{1y} \\ z_{2x} \\ z_{2y} \\ z_{3x} \\ z_{3y} \end{bmatrix} + M_z R_2$$

$$A_1 = -F_x \sin \phi + F_y \cos \phi$$

$$A_2 = -F_x \cos \phi - F_y \sin \phi$$

$$A_3 = -F_x R_1 \sin(R_1 \phi) + F_y R_1 \cos(R_1 \phi) \quad (3)$$

$$A_4 = -F_x R_1 \cos(R_1 \phi) - F_y R_1 \sin(R_1 \phi)$$

$$A_5 = -F_x R_2 \sin(R_2 \phi) + F_y R_2 \cos(R_2 \phi)$$

$$A_6 = -F_x R_2 \cos(R_2 \phi) - F_y R_2 \sin(R_2 \phi)$$

For a given set of kinematic parameters and a specified end-effector load profile, the torque required to equilibrate the load profile is completely determined. However, the contribution of the spring torques can alter the actual actuation requirement and can potentially allow for the exact matching of the desired actuation torque curve. This is the crux of our adopted approach.

We introduce the following notation in order to calculate the spring torques. Let θ_i be the absolute initial configuration of each joint, Ω_i be the absolute configuration of each joint at which the springs are assembled, and ϕ be the relative displacement of the first link from its initial configuration to the current configuration. Then, β_i , the angular extension of each spring, can be written as

$$\beta_1 = \theta_1 + \phi - \Omega_1 \quad (4)$$

$$\beta_i = [(\theta_i + R_{i-1} \phi - \Omega_i) - (\theta_{i-1} + \phi - \Omega_{i-1})] \quad \forall i > 2$$

Thus, the overall contribution of the internal spring torques can be expressed as

$$T_{\text{Spr}} = k_1(\theta_1 + \phi - \Omega_1) + k_2[(R_1 - 1)\phi + (\theta_2 - \theta_1) + (\Omega_1 - \Omega_2)](R_1 - 1) + k_3[(R_2 - R_1 + 1)\phi + (\theta_3 - \theta_2 + \theta_1) + (\Omega_2 - \Omega_3 - \Omega_1)] \times (R_2 - R_1 + 1)$$

$$= [k_1 + k_2(R_1 - 1)^2 + k_3(R_2 - R_1 + 1)^2]\phi + k_1(\theta_1 - \Omega_1) + k_2(R_1 - 1)[(\theta_2 - \theta_1) + (\Omega_1 - \Omega_2)] + k_3(R_2 - R_1 + 1)[(\theta_3 - \theta_2 + \theta_1) + (\Omega_2 - \Omega_3 - \Omega_1)] \quad (5)$$

Nominally, a system with three springs requires the specification of six variables— $k_1, k_2, k_3, \Omega_1, \Omega_2, \Omega_3$. However, we note that the spring torque equation can also be rewritten in terms of the relative angular motion of the first joint as a linear equation as

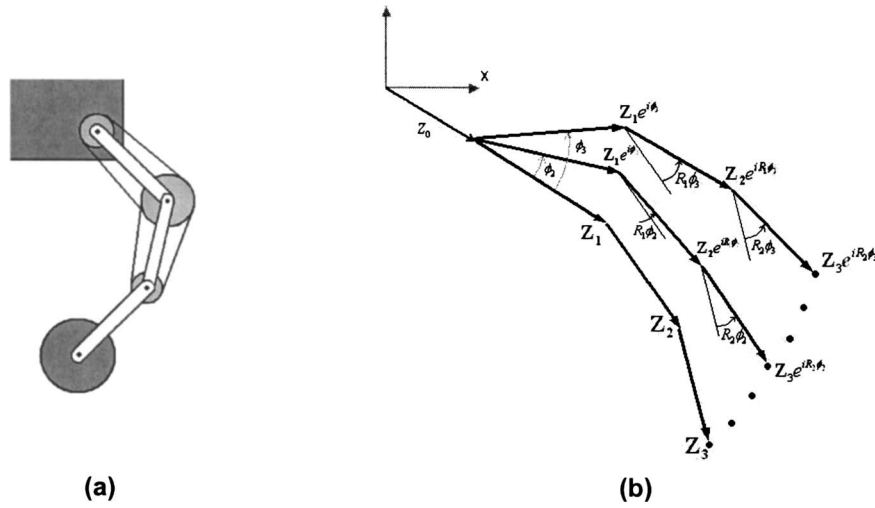


Fig. 9 (a) Three-link SDCSC-based leg-wheel design, and (b) the corresponding kinematic diagram

$$T_{Spr}(\phi) = A\phi + B = A \left[\theta_1 + \phi + \left(\frac{B - A\theta_1}{A} \right) \right] \quad (6)$$

with the implication that all linear torsional springs (attached at the various joints of an SDCSC mechanism) can in fact be replaced by a single equivalent lumped torsional spring with spring constant $K_{eq}=A$ and an initial unloaded configuration of $\Omega_{eq} = -\frac{B-A\theta_1}{A}$. The spring constants k_1, k_2, k_3 can then be related back to A and B through the following underdetermined system

$$\begin{bmatrix} A \\ B \end{bmatrix} = [S] \begin{bmatrix} k_1 \\ k_2 \\ k_3 \end{bmatrix} = \begin{bmatrix} -1 & -(R_1 - 1)^2 & -(R_2 - R_1 + 1)^2 \\ s_{21} & s_{22} & s_{23} \end{bmatrix} \begin{bmatrix} k_1 \\ k_2 \\ k_3 \end{bmatrix} \quad (7)$$

where

$$s_{21} = -(\theta_1 - \Omega_1)$$

$$s_{22} = -(R - 1)[(\theta_2 - \theta_1) + (\Omega_1 - \Omega_2)]$$

$$s_{23} = -(R_2 - R_1 + 1)[(\theta_3 - \theta_2 + \theta_1) + (\Omega_2 - \Omega_3 - \Omega_1)]$$

Since there are more unknowns than equations, we note that a secondary optimization may also be created in terms of the k_i 's. However, a naive (but direct) solution for the unknown spring constants using pseudo inverse of $[S]$ matrix may give rise to negative k_i 's. Such infeasible values for k_i 's can be avoided by adding components from the nullspace to ensure positive values for all k_i 's. Regardless, it is reasonably obvious that the designer has considerable freedom to either (i) determine the best unloaded configuration for a given k_1, k_2 , and k_3 ; or alternately (ii) vary the initial unloaded configuration to enable suitable selection of a spring constant. See [21] for further details.

The desired torque curve is assumed to be given as a function of the actuated joint displacement as discussed in Sec. 2.3. However, from Eq. (6) we note that we only have two design variables for use in the static synthesis process (regardless of number of links of SDCSC mechanism) which can be used in the following ways:

- two static precision points and no free choices (presented below in Sec. 3.2.1);
- one static precision point and using one of the variables as a free choice (not presented); and
- no static precision points but with both variables as free choices (in Sec. 3.2.2).

3.2.1 Two Static Precision Points and No Free Choices. For a two static precision synthesis torque problem, the equivalent spring parameters, A and B , are calculated to satisfy the specified torques, $T_1^d(\phi_i)$ at the precision points, ϕ_i as

$$\begin{bmatrix} A \\ B \end{bmatrix} = \begin{bmatrix} \phi_1 & 1 \\ \phi_2 & 1 \end{bmatrix}^{-1} \begin{bmatrix} T_1^d(\phi_1) - T_{Ext}(\phi_1) \\ T_1^d(\phi_2) - T_{Ext}(\phi_2) \end{bmatrix} \quad (8)$$

By combining this calculation with Eq. (7), values of the physical springs can then be determined.

The effect of the suitable selection of precision points is illustrated in Fig. 11. The postsynthesis torque profile is guaranteed to match the desired torque profile at the precision points in both cases. However, in Fig. 11(a) the appropriate selection of precision points also gives rise to a good match of the desired torque profile as compared to Fig. 11(b). Further, as seen in Fig. 11(b), it

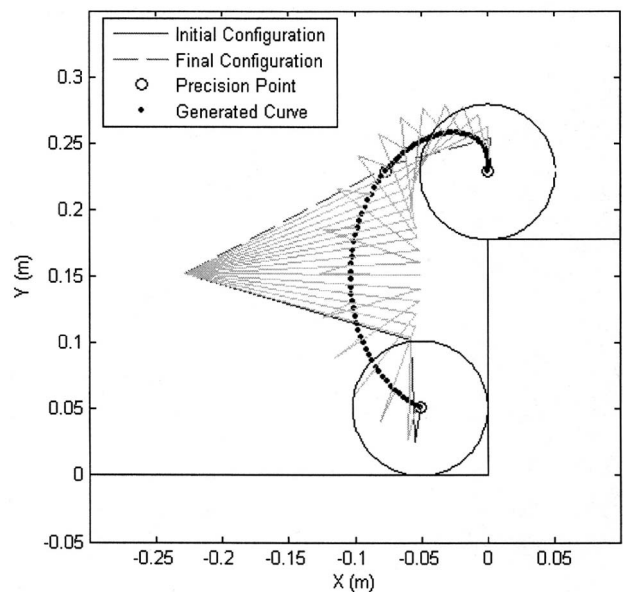


Fig. 10 Candidate SDCSC articulated leg-wheel subsystem surmounting the ideal step profile

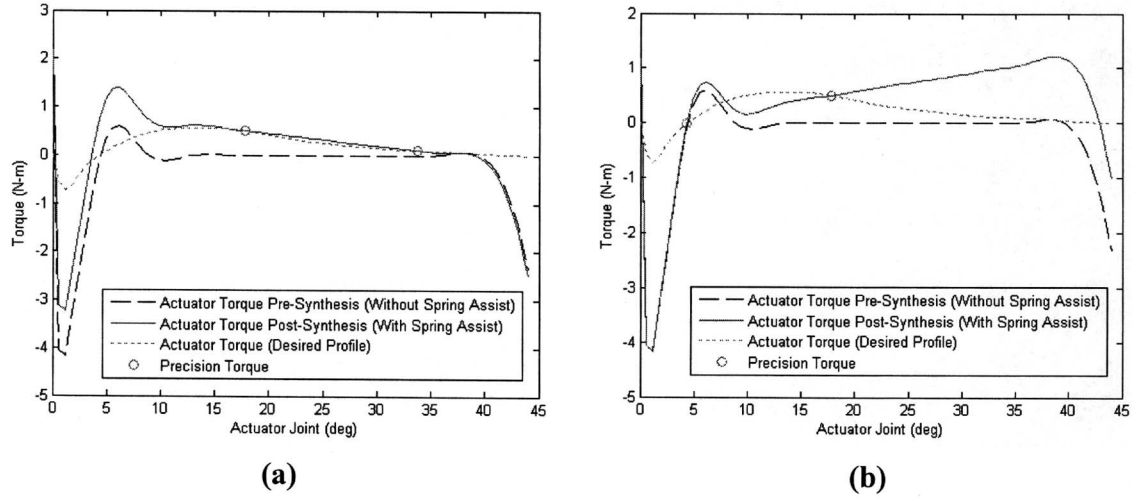


Fig. 11 Actuator torque profiles of the three-link SDCSC configuration with two static precision torques

is possible to use precision torque requirements to design the (unstable) equilibrium position that separates the different basins of attraction.

3.2.2 No Static Precision Points and Using Both Variables as Free Choices. A variety of objective functions, including force consideration in their objective, can be employed as noted in [17,18]. We will employ the least-squares matching of a desired torque profile as the proposed objective in our work. The torque at Joint 1, T_1 , is written as

$$T_1 = T_{\text{Ext}} - T_{\text{Spr}} = T_{\text{Ext}} - (A\phi + B) \quad (9)$$

and using a and b as the design variables, the optimization problem can be stated as

$$\min_{a,b} \sum_{k=1}^{N_e} (T_1^{\text{des}} - T_1^{\text{act}})^2 \quad (10)$$

Figure 12 shows the result of such an optimization. Observe that the pre-optimized actuator torque is the torque that would have been exerted prior to the addition of the spring assist and is the same across Figs. 11 and 12. The final optimized torque profile, with spring assist, now matches the desired torque profile in the least-squares sense without guaranteeing an exact match at any position. However, we note that since the spring torques of an SDCSC-based design form a linear function, the actual torque profile is not able to match complex desired torque profiles.

4 Design/Synthesis of Four-Bar Leg-Wheel Mechanism

The four-bar linkage has found ubiquitous applicability in machinery applications due to its extreme versatility in modulating transmitted motions and forces. We will similarly exploit this versatility in designing an articulated leg-wheel system based on the four-bar configuration.

4.1 Kinematic Synthesis. The dyadic synthesis approach, outlined in greater detail in [19,20], is adopted for generating the kinematic constraint equations. As in the case of the SDCSC mechanism, the number of feasible precision points is limited. The four-bar linkage can be synthesized by closed-form methods up to five precision points for the path-following problem. The four or more precision point synthesis problems involve the solutions of nonlinear equations—hence we consider only the two or three pre-

cision point cases (see Fig. 13). In the latter case, the overall kinematic design selection problem may be expressed in the form of a constrained optimization problem as

$$\min_{\alpha_2, \alpha_4, \alpha'_2, \alpha'_4, \beta, \beta'} \sum_{k=1}^N [(P_{x,k} - Q_{x,k})^2 + (P_{y,k} - Q_{y,k})^2] \quad (11)$$

subject to

$$\begin{bmatrix} \mathbf{Z}_2 \\ \mathbf{Z}_6 \\ \mathbf{Z}_4 \\ \mathbf{Z}_5 \end{bmatrix} = \begin{bmatrix} (e^{i\alpha_2} - 1) & (e^{i\beta} - 1) & 0 & 0 \\ (e^{i\alpha'_2} - 1) & (e^{i\beta'} - 1) & 0 & 0 \\ 0 & 0 & (e^{i\alpha_4} - 1) & (e^{i\beta} - 1) \\ 0 & 0 & (e^{i\alpha'_4} - 1) & (e^{i\beta'} - 1) \end{bmatrix}^{-1} \times \begin{bmatrix} \mathbf{R}_2 - \mathbf{R}_1 \\ \mathbf{R}_3 - \mathbf{R}_1 \\ \mathbf{R}_2 - \mathbf{R}_1 \\ \mathbf{R}_3 - \mathbf{R}_1 \end{bmatrix}$$

$$\alpha_{2,\min} \leq \alpha_2 \leq \alpha_{2,\max}, \quad \alpha_{4,\min} \leq \alpha_4 \leq \alpha_{4,\max}, \quad \beta_{\min} \leq \beta \leq \beta_{\max}$$

$$\alpha'_{2,\min} \leq \alpha'_2 \leq \alpha'_{2,\max}, \quad \alpha'_{4,\min} \leq \alpha'_4 \leq \alpha'_{4,\max}, \quad \beta'_{\min} \leq \beta' \leq \beta'_{\max}$$

Each link vector is modeled in complex number form as $Z_k = Z_{kx} + Z_{ky} = z_k e^{i\theta_k}$. The design variables in the optimization problem are the incremental angles of the input, follower, and coupler links at the second precision point ($\alpha_2, \alpha_4, \beta$) and the third precision point ($\alpha'_2, \alpha'_4, \beta'$). $\mathbf{P}_k = P_{x,k} + iP_{y,k}$ is the generated end-effector position and $\mathbf{Q}_k = Q_{x,k} + iQ_{y,k}$ is the desired end-effector position. Among the possible configurations, an acceptable configuration of the four bar is listed in Table 2. Figure 14 shows the four-bar at the initial and final configurations, along with the path followed by the wheel axle.

4.2 Kinetostatic Synthesis. As in the case of the SDCSC-based design, the expression for the torque due to external sources at the driving joint T_{Ext} and the spring torque T_{Spr} can be calculated from the expression for virtual work in the system [21] as

Table 2 Parameters of the optimized four bar

Parameter	Value	Parameter	Value
Z_{0x}	-0.2890 m	Z_{0y}	0.3380 m
Z_{1x}	0.1750 m	Z_{1y}	-0.1110 m
Z_{2x}	0.1160 m	Z_{2y}	0.0989 m
Z_{3x}	-0.0581 m	Z_{3y}	-0.2900 m
Z_{4x}	-0.1170 m	Z_{4y}	-0.0806 m
Z_{5x}	0.1800 m	Z_{5y}	0.0958 m
Z_{6x}	0.1220 m	Z_{6y}	-0.3860 m
α_2	89.5 deg	α'_2	180 deg

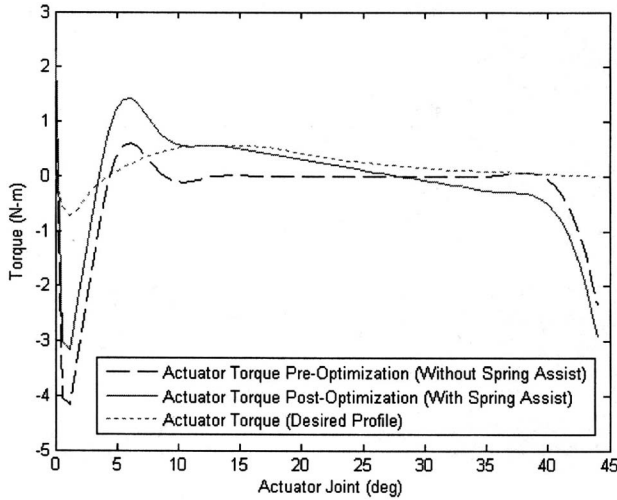


Fig. 12 Actuator torque optimization for a three-link SDCSC configuration

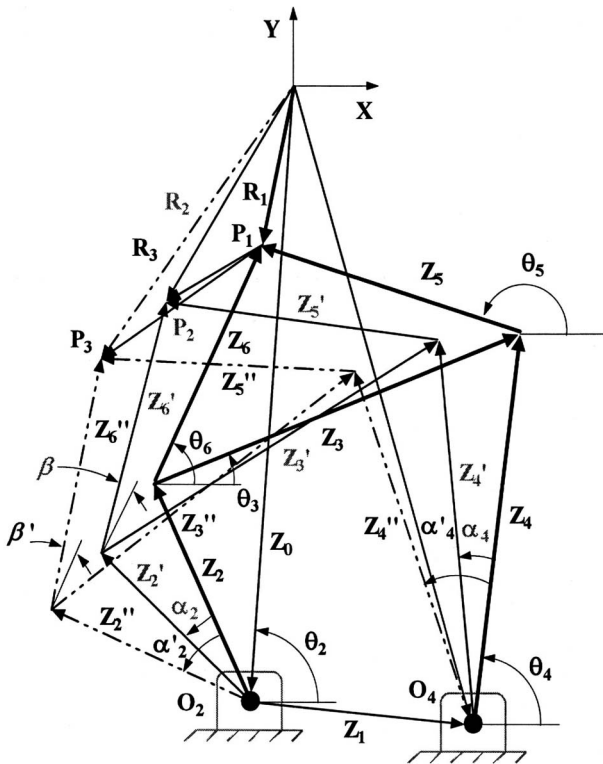


Fig. 13 Nomenclature of the four-bar linkage at three precision positions

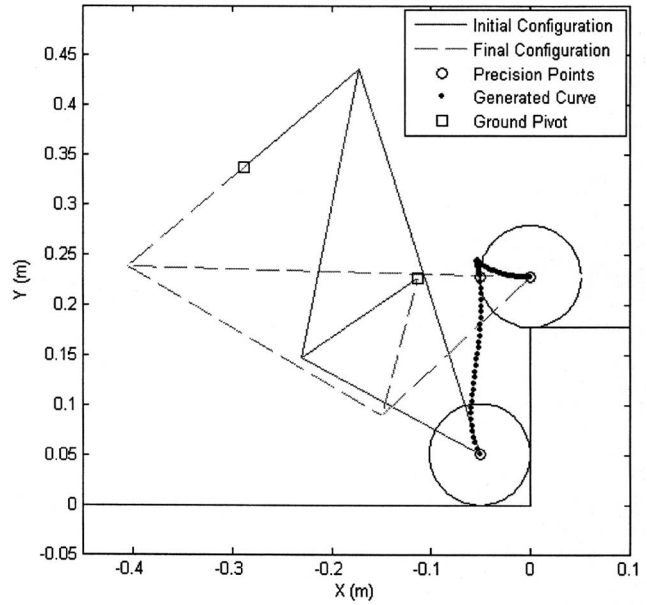


Fig. 14 Kinematic configuration of four bar for desired step trajectory

$$T_{Ext} = -F_x[z_2 \sin \theta_2 + A_1 z_6 \sin(\theta_3 + \gamma_6)] + F_y[z_2 \cos \theta_2 + A_1 z_6 \cos(\theta_3 + \gamma_6)] + A_1 M \quad (12)$$

where

$$A_1 = \frac{z_2 \sin(\theta_4 - \theta_2)}{z_3 \sin(\theta_3 - \theta_4)}, \quad A_2 = \frac{z_2 \sin(\theta_3 - \theta_2)}{z_4 \sin(\theta_3 - \theta_4)}$$

The spring equation can be written in terms of relative angular motion of the three joints as

$$T_{Spr} = -k_2(\theta_{2,initial} + \alpha_2 - \Omega_2) - k_3(A_1 - 1)[(\theta_{3,initial} + \beta - \Omega_3) - (\theta_{2,initial} + \alpha_2 - \Omega_2)] - k_4 A_2(\theta_{4,initial} + \alpha_4 - \Omega_4) - k_5(A_1 - A_2) \times [(\theta_{3,initial} + \beta - \Omega_3) - (\theta_{4,initial} + \alpha_4 - \Omega_4)] \quad (13)$$

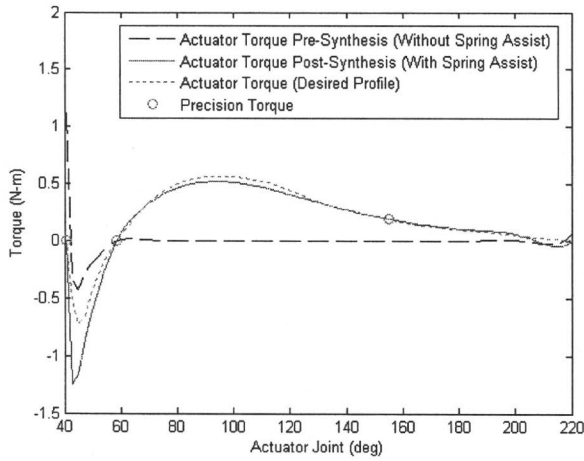
which may be simplified to show the linearity of the spring torque expression as

$$T_{Spr} = a\alpha_2 + b\alpha_4 + c\beta + d \quad (14)$$

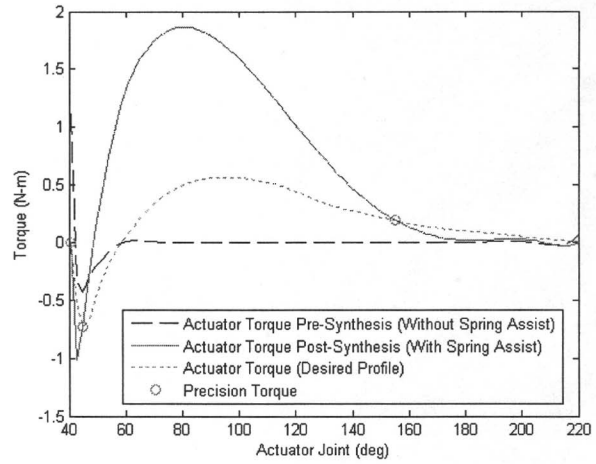
In general, the total required actuation, $T_{act} = T_{Ext} - T_{Spr}$, depends on both the selected configuration as well as the spring parameters. As in the previous section, we adopt a decoupled approach in which the kinematic configuration is predetermined in a kinematic design-optimization stage. The four design variables (a, b, c, d) need to be selected to permit matching the desired static torque profile. While many cases are possible based on the number of precision points selected, we will examine the following two cases:

- four static precision points and no free choices (in Sec. 4.2.1); and
- no static precision points and using all four variables as free choices (in Sec. 4.2.2).

4.2.1 Four Static Precision Points and No Free Choices. For a four static precision torque problem, the equivalent spring parameters may be calculated by substituting precision torques—the specified torques, $T_i^d(\phi_{2i})$, at the precision points, α_{2i} in Eq. (13).



(a)



(b)

Fig. 15 Actuator torque profiles of the four-bar configuration with four static precision torques

$$\begin{bmatrix} a \\ b \\ c \\ d \end{bmatrix} = \begin{bmatrix} \alpha_{2,1} & \alpha_4(\alpha_{2,1}) & \beta(\alpha_{2,1}) & 1 \\ \alpha_{2,2} & \alpha_4(\alpha_{2,2}) & \beta(\alpha_{2,2}) & 1 \\ \alpha_{2,3} & \alpha_4(\alpha_{2,3}) & \beta(\alpha_{2,3}) & 1 \\ \alpha_{2,4} & \alpha_4(\alpha_{2,4}) & \beta(\alpha_{2,4}) & 1 \end{bmatrix}^{-1} \begin{bmatrix} T_{\text{Joint},1} - T_{\text{Ext}}(\alpha_{2,1}) \\ T_{\text{Joint},2} - T_{\text{Ext}}(\alpha_{2,2}) \\ T_{\text{Joint},3} - T_{\text{Ext}}(\alpha_{2,3}) \\ T_{\text{Joint},4} - T_{\text{Ext}}(\alpha_{2,4}) \end{bmatrix} \quad (15)$$

The desired k_i and corresponding Ω_i can be determined by solving

$$\begin{bmatrix} k_2 \\ k_3 \\ k_4 \\ k_5 \end{bmatrix} = \begin{bmatrix} -1 & (A_1 - 1) & 0 & 0 \\ 0 & 0 & -A_2 & (A_1 - A_2) \\ 0 & -(A_1 - 1) & 0 & -(A_1 - A_2) \\ m_{41} & m_{42} & m_{43} & m_{44} \end{bmatrix}^{-1} \begin{bmatrix} a \\ b \\ c \\ d \end{bmatrix}$$

$$m_{41} = -(\theta_{2,\text{initial}} - \Omega_2)$$

$$m_{42} = -(A_1 - 1)[(\theta_{3,\text{initial}} - \Omega_3) - (\theta_{2,\text{initial}} - \Omega_2)]$$

$$m_{43} = -A_2(\theta_{4,\text{initial}} - \Omega_4)$$

$$m_{44} = -(A_1 - A_2)[(\theta_{5,\text{initial}} - \Omega_5) - (\theta_{4,\text{initial}} - \Omega_4)] \quad (16)$$

Note that as in the SDCSC-based design, Eq. (16) gives us freedom for selection of spring constants. For example, noting that commercially available springs have restricted values of spring constants, a secondary optimization to minimize them can be easily performed using spring preloads as design variables.

Note that this obtained torque profile corresponds to the previously determined kinematic trajectory of Fig. 14. Changing the kinematic trajectory will alter the torque profile and can serve as an additional useful source of freedom for the designer. Similar to the discussion in Sec. 3.2.1 it is now possible to generate an exact match of the desired torque profile at the precision points. In general, the match is better even for more complex desired torque profiles since we can specify more precision points. Nevertheless, the selection of suitable locations for the precision points (the designer's prerogative) still plays a significant role as seen in Figs. 15(a) and 15(b).

4.2.2 No Static Precision Points and Using Four Variables as Free Choices. As in the case of SDCSC, we minimize the discrepancy between the desired and actual torque profiles required to generate the motion. Optimization is carried out over the many candidate solutions by varying a, b, c, d in Eq. (14) as the design variables to find the best solution. Figure 16 shows the result of

such an optimization. In contrast to the torque optimization with the SDCSC-based design seen in Fig. 12, we see that a four-bar based design is better able to match complex torque profiles in situations where nonanthropomorphic configurations can be deployed.

5 Conclusion

In this paper, we considered two alternate designs of articulated leg-wheel subsystems to modulate the motion and force interactions between the ground and the chassis and thereby enable vehicle systems to locomote in difficult environments and rough terrain. We focused our attention on employing single degree-of-freedom intermediate articulations and passive mechanical implementation in selecting the four-bar-based and the SDCSC-based design configurations. We emphasized the design customization and adaptation of these two designs to match desired kinetostatic specifications—surmounting a candidate obstacle profile while supporting a desired end-effector load. Suitable selection of both *kinematic* parameters, such as the link lengths and initial configuration, as well as *static* parameters, such as spring constants and their preloads, proved critical. We highlighted a systematic ap-

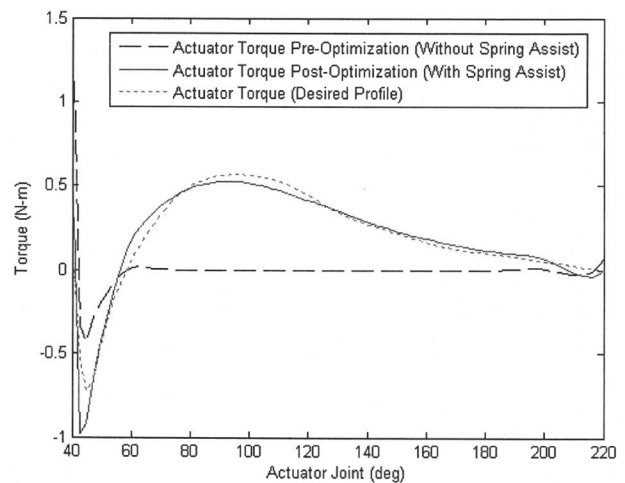


Fig. 16 Actuator torque optimization for the four-bar configuration

proach for the selection of both sets of mechanism design parameters that allowed them to surmount significant terrain obstacles while reducing the actuation requirements. In general, the four-bar based design was better able to match both the desired kinematic and static specifications. However, in certain situations the anthropomorphic (and more compact) configuration of the SDCSC-based design provides better end-effector reach and clearance as compared to the four-bar based design.

Acknowledgment

We gratefully acknowledge the financial support from the National Science Foundation CAREER Award (IIS-0347653) and the New York State Center for Engineering Design and Industrial Innovation (NYSCEDII).

References

[1] Hacot, H., Dubowsky, S., and Bidaud, P., 1998, "Modeling and Analysis of a Rocker-Bogie Planetary Exploration Rover," *Proceedings of the 12th CISM-IFTOMM Symposium (RoManSy 98)*, July 6–9, Paris, France.

[2] Hacot, H., 1998, "Analysis and Traction Control of a Rocker-Bogie Planetary Rover," M.S. thesis, Department of Mechanical Engineering, MIT, Cambridge, MA.

[3] Siegwart, R., Lamon, P., Estier, T., Lauria, M., and Piguat, R., 2002, "Innovative Design for Wheeled Locomotion in Rough Terrain," *Robotics and Autonomous Systems*, **40**(2), pp. 151–162.

[4] Wettergreen, D., Bualat, M., Christian, D., Schwehr, K., Thomas, H., Tucker, D., and Zbinden, E., 1997, "Operating Nomad During the Atacama Desert Trek," *Proceedings of Field and Service Robotics Conference*, December 7–10, Canberra, Australia.

[5] Halme, A., Leppänen, I., and Salmi, S., 1999, "Development of Workpartner-Robot—Design of Actuating and Motion Control System," *2nd International Conference on Climbing and Walking Robots (CLAWAR 99)*, Portsmouth, England, Wiley Publishers, September 13–15, pp. 657–666.

[6] Halme, A., Leppänen, I., Montonen, M., and Ylönen, S., 2001, "Robot Motion by Simultaneous Wheel and Leg Propulsion," *Fourth International Conference on Climbing and Walking Robots (CLAWAR'01)*, Karlsruhe, Germany, Profes-

sional Engineering, Publishing Ltd., September 25–27, pp. 1013–1020.

[7] Hirose, S., 2000, "Super Mechano-System," *International Symposium on Experimental Robotics (ISER2000)*, Daniela Rus, ed., Springer-Verlag, December 10–13, Honolulu, HI.

[8] Song, S.-M., and Waldron, K., 1988, *The Adaptive Suspension Vehicle*, MIT Press, Cambridge, MA.

[9] Berns, K., 2002, *The Walking Machine Catalogue*, URL: <http://www.walking-machines.org/>.

[10] Bekker, M., 1956, *Theory of Land Locomotion: The Mechanics of Vehicle Locomotion: The Mechanics of Vehicle Mobility*, The University of Michigan Press, Ann Arbor, MI.

[11] Bekker, M., 1969, *Introduction to Terrain Vehicle Systems*, The University of Michigan Press, Ann Arbor, MI.

[12] Wong, J., 1989, *Terramechanics and Off-road Vehicles*, Elsevier, Amsterdam, Netherlands.

[13] Sreenivasan, S. V., and Waldron, K. J., 1996, "Displacement Analysis of an Actively Articulated Wheeled Vehicle Configuration With Extensions to Motion Planning on Uneven Terrain," *ASME J. Mech. Des.* **118**(2), pp. 312–320.

[14] Endo, G., and Hirose, S., 1999, "Study on Roller-Walker: System Integration and Basic Experiments," *Proceedings of 1999 IEEE International Conference on Robotics and Automation*, Detroit, Michigan, May 10–15, pp. 2031–2037.

[15] Endo, G., and Hirose, S., 2000, "Study on Roller-Walker (Multi-Mode Steering Control and Self-Contained Locomotion)," *Proceedings of 2000 IEEE International Conference on Robotics and Automation*, San Francisco, CA, April 24–28, pp. 2808–2814.

[16] Hiller, M., and German, D., 2002, "Manoeuvrability of the Legged and Wheeled Vehicle ALDURO in Uneven Terrain with Consideration of Nonholonomic Constraints," *Proceeding off 2002 International Symposium on Mechatronics (ISOM 2002)*, March 21–22, Chemnitz, Germany.

[17] Krovi, V., 1998, "Design and Virtual Prototyping of User-Customized Assistive Devices," Ph.D. thesis, University of Pennsylvania, Philadelphia, PA.

[18] Krovi, V., Ananthasuresh, G. K., and Kumar, V., 2002, "Kinematic and Kinestatic Synthesis of Planar Coupled Serial Chains," *ASME J. Manuf. Sci. Eng.* **124**(2), pp. 143–155.

[19] Sandor, G., and Erdman, A. G., 1984, *Advanced Mechanism Design: Analysis and Synthesis*, Prentice-Hall, International Englewood Cliffs, NJ, Vol. 2.

[20] Norton, R., 2004, *Design of Machinery*, 3rd ed., McGraw-Hill, New York.

[21] Jun, S. K., 2004, "Kinestatic Design of an Articulated Leg-Wheel Locomotion Subsystem," M.S. thesis, State University of New York at Buffalo, Buffalo, NY.